Modeling Rice Growth and Yield using Integrated Remote Sensing Data on Google Earth Engine

Boonma, R., Suwanprasit, C.* and Homhuan, S.
Department of Geography, Faculty of Social Sciences, Chiang Mai University 50200, Thailand
E-mail: Raweewan_b@cmu.ac.th, chanida.suwanprasit@cmu.ac.th,* sakda.homhuan@cmu.ac.th
Corresponding Author

DOI: https://doi.org/10.52939/ijg.v20i11.3693

Abstract
Assessing the growth stages, health, and yield of rice is crucial for agriculture, economy, sustainability, and food security. Such assessments provide valuable insights for farmers to optimize agricultural practices, effectively manage pests and diseases, and enhance crop management, leading to improved yields and efficient resource management. This study focuses on paddy fields in Buak Khang sub-district, San Kamphaeng district, Chiang Mai, Thailand, with the objective of developing models to assess rice growth stages, evaluate rice health using the NDVI, and model rice yield using Sentinel-2 MSI and Sentinel-1 SAR (VV and VH polarizations) satellite imagery. The study was conducted during the rainy season of 2023 (June-November). Various parameters were identified to establish correlations and develop models, with field data collected to validate the models. The study yielded three models for rice growth stage assessment, with the best model achieving an R^2 of 0.67. Monitoring rice health revealed that on September 21, the NDVI values ranged between 0.51 and 0.91, indicating optimal growth conditions and healthy crops. Similarly, three models were developed for yield estimation, with the best model achieving an R^2 of 0.51. Validation showed that the growth stage model had a Kappa coefficient of 0.80, while the yield estimation model had a RMSE of 0.887 kg/m². These models, demonstrating high accuracy, provide a robust framework for agricultural agencies to develop effective agricultural policies.

Keywords: Estimating Rice Yield, Google Earth Engine (GEE), Growth Stages, Linear Regression, Rice Phenology

1. Introduction

Rice is a staple food for more than three billion people worldwide and is cultivated on approximately 12% of the world's arable land. However, over 88% of production occurs in Asian countries [1]. In Thailand, rice is a crucial economic crop, being the country's primary agricultural export and covering the largest cultivation area, accounting for 46.1% of all agricultural land. In northern Thailand, Chiang Mai Province ranks among the top regions for rice cultivation. Most rice fields in Chiang Mai are located in San Kamphaeng District, which benefits from rivers and irrigation, providing farmers with a year-round water supply for rice farming. Buak Khang Subdistrict in San Kamphaeng District is one of the areas participating in a large-scale rice farming project. Rice farmers have organized themselves into groups to create a network for negotiating rice prices with middlemen. They have also received support in terms of agricultural tools and equipment from relevant agencies, which has significantly contributed to reducing production costs, improving the quality of rice to higher standards, and substantially increasing rice yields in the area. However, there are many instances where farmers face crop yields that do not meet expectations, even when the crops are well-managed [2]. Thus, accurately and timely tracking rice growth stages, predicting growth stage classifications, monitoring crop health, and forecasting yields can significantly enhance farmers' decision-making regarding production cost management, such as specific fertilizer application rates [3]. These data can also be crucial for assessing food security [4] and assisting relevant agencies in planning production and marketing strategies [5].

However, field data collection and monitoring rice growth stages in agricultural areas are labor-intensive, time-consuming, and costly. In this context, remote sensing technology through satellites offers high-frequency, accurate, cost-effective, and dynamic data for effective mapping, monitoring, and management [6].

Remote sensing technology plays a significant role in agriculture and ecology at the regional level. Integrating Synthetic Aperture Radar (SAR) and optical data provides extensive spatial and temporal information, essential for monitoring rice growth stages, assessing crop health, and forecasting yields. SAR data are not influenced by clouds or sunlight, making them ideal for tracking and predicting rice growth stages in areas without cloud-free optical imagery [7]. Concurrently, optical data from Sentinel-2 provide Multispectral Instrument (MSI) reflectance data, which can be used to determine the time series of vegetation indices in cultivated areas [8]. However, processing satellite imagery for large areas and multiple time periods can be challenging. The Google Earth Engine (GEE) platform facilitates access and analysis of Earth science data, streamlining the processing of large-scale, multi-temporal satellite data, such as those from Sentinel-1 and Sentinel-2, Landsat 4, 5, 7, and 8, and MODIS [9]. Previous studies have focused on yield estimation by analyzing the phenological stages of rice using regression algorithms such as the cumulative NDVI and EVI based Logistic regression curves (CNELRC), Partial Least Squares Regression (PLSR), Support Vector Regression (SVR), Random Forest Regression (RFR), and Back Propagation Neural Networks (BPNN) [10] and [11]. For instance, studies have used vegetation indices to estimate yield at the pixel level using hyperspectral imagery from UAV platforms [12] with multiple linear regression (MLR) algorithms [13]. Other studies include spatial yield estimation based on MODIS and Sentinel-1 SAR data [14] and the installation of weather station poles equipped with RGB cameras to study rice phenology [15]. However, these studies often have limitations due to high costs and are sometimes restricted to yield estimation from rice phenological stages without mapping growth stages or assessing crop health. This study aims to evaluate rice growth stages, assess crop health, and estimate yields using MLR techniques combined with optical sensor data and SAR data from Sentinel-1 and Sentinel-2 satellite images processed on the GEE platform.

2. Materials and Methods

2.1 Study Area

This study was conducted in Buak Khang Subdistrict, San Kamphaeng District, Chiang Mai Province, Thailand, located at coordinates 18°43′51.1″N 99°04′33.4″E and 18°40′06.9″N 99°08′26.8″E (Figure 1). The area covers approximately 27.85 square kilometers.

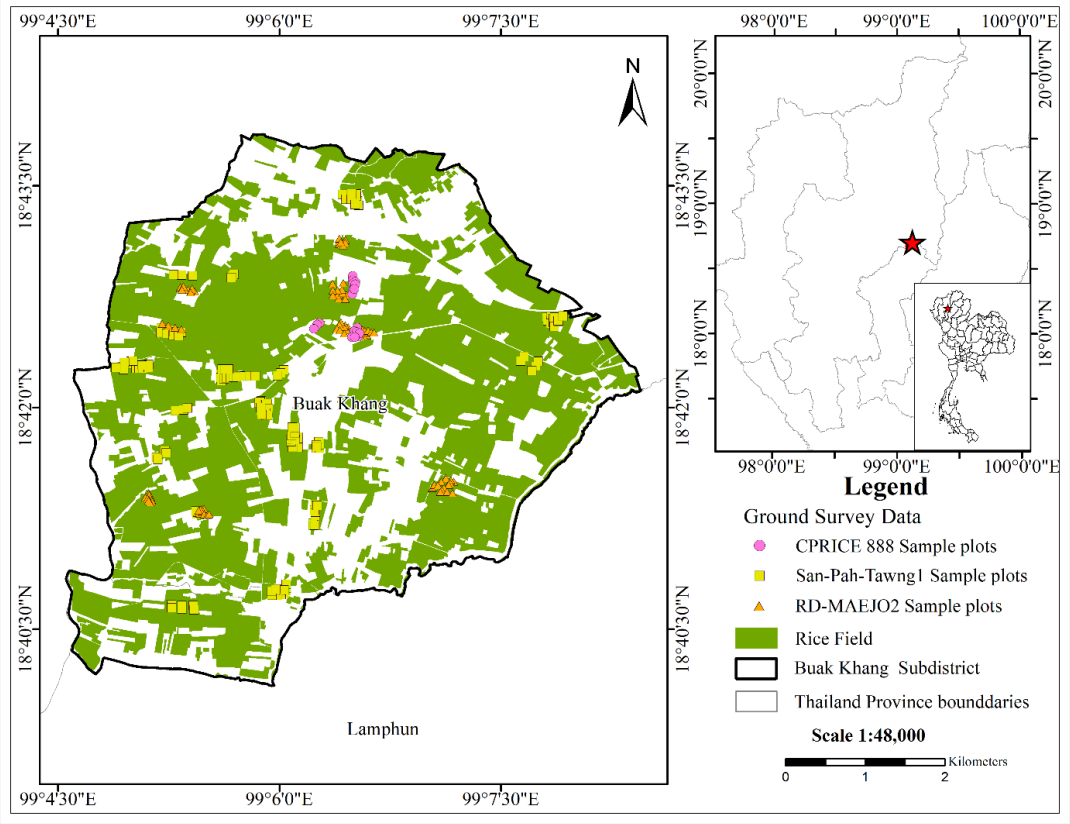

Figure 1: Buak Khang subdistrict, San Kamphaeng district, Chiang Mai province

The local population primarily engages in agriculture, such as rice farming, tobacco cultivation, vegetable gardening, and livestock farming. Due to the region's extensive plains and several significant rivers flowing through it, residents have year-round access to water for agricultural activities. This study focuses on rice cultivation areas in Buak Khang Subdistrict, which total 17.901 square kilometers. Field surveys revealed that most farmers in the large-scale agriculture group cultivate various rice varieties, such as San-Pah-Tawng1, RD-MAEJO2, and CPRICE 888.

2.2 Datasets

2.2.1 Satellite imagery datasets

This study uses Sentinel-1 and Sentinel-2 satellite imagery for analysis, covering the period from June to November 2023, which corresponds to the initial rice planting season in the study area. The Sentinel-1 C-Band imagery from descending orbits, featuring *VH* and *VV* polarizations, has a spatial resolution of 10 meters and the capability to capture images both day and night and in all weather conditions. This makes it suitable for tracking the phenology and growth stages of rice in the study area. For the Sentinel-2 MSI satellite imagery, bands Blue, Green, Red, Near Infrared (NIR), and Short-Wave Infrared (SWIR) with spatial resolutions ranging from 10 to 20 meters were used to analyze vegetation indices. These indices help assess the crop health and estimate the yield in the study area. Each image had less than 30% cloud cover. All analyses were conducted on the GEE platform.

2.2.2 Field survey data

In this study, field surveys and data collection were conducted in collaboration with farmers participating in a large-scale rice cultivation project. The collected data included the number of days after rice plantings, rice varieties planted, and yield quantities. The sample plots were selected using stratified random sampling, based on the following criteria: 1) rice cultivation areas of 8,000 square meter or more, 2) similar planting periods (June - November 2023), and 3) cultivation of CPRICE 888, San-Pah-Tawng1, and RD-MAEJO2 rice varieties. The survey identified a total of 44 eligible sample plots within the study area. The number of sample plots for each rice variety varied based on the farmers' choice of rice variety. Since most farmers in the area preferred to cultivate San-Pah-Tawng1, there were more sample plots for this variety compared to others. Additionally, this study aims to collect sample points within the plots to comprehensively cover the study area. The sample points will use stratified random sampling based on the size of the selected sample plots. For sample plots sized 8,000 to 16,000 square meter, there will be 3-4 sample points; for plots sized 16,000 to 24,000 square meter, there will be 6 sample points; and for plots larger than 24,000 square meter, there will be 9 sample points. All sample points must be distributed throughout the sample plots. The sample points for each rice variety are as follows: 30 for CPRICE 888, 111 for San-Pah-Tawng1, and 48 for RD-MAEJO2, resulting in a combined total of 189 points.

2.3 Rice phenology

This research focuses on studying the phenology of rice in Buak Khang Subdistrict, examining the phenology of three rice varieties from planting to harvest (June - November 2023). The growth stages are divided into three phases: Vegetative Phase (0 - 60 days), Reproductive Phase (60 - 90 days), and Ripening Phase (90 - 135 days) [16]. The study combines field data collection with remote sensing data from Sentinel-1 SAR and Sentinel-2 satellite imagery to track the phenology of rice at different times. Factors influencing rice growth include temperature, water availability, nutrient management, light duration, and genetic factors. Due to the small size of the study area, the physical characteristics are similar, and it is an irrigated area. The three rice varieties used in this study are glutinous rice that is not sensitive to photoperiod. Each variety has specific characteristics as follows: San-Pah-Tawng1 is resistant to rice blast and bacterial leaf blight, making it suitable for year-round cultivation with a harvest period of approximately 130–135 days. RD-MAEJO 2 is resistant to bacterial leaf blight and brown planthopper, allowing it to be grown in both the main and off-seasons, with a harvest time of about 135 days in the main season and 146 days in the off-season. CPRICE 888 is a glutinous rice variety suitable for year-round cultivation, particularly in irrigated areas in Northern Thailand, with a harvest period ranging from 130 days, making it flexible and responsive to farmers' needs. However, field surveys revealed that large-scale rice farmers use the same fertilizer formula and regularly monitor soil nutrients, resulting in similar growth patterns across all three rice varieties. Consequently, this study adopts an overall approach rather than a variety-specific analysis.

Figure 2 shows the NDVI vegetation index values and growth stages of three rice varieties: San-Pah-Tawng1, RD-MAEJO2, and CPRICE 888, cultivated in Buak Khang Subdistrict during the 2023 planting season. Previous studies indicate that during the vegetative phase (0-60 days), the NDVI values range from less than 0.17 and gradually increase to approximately 0.52.

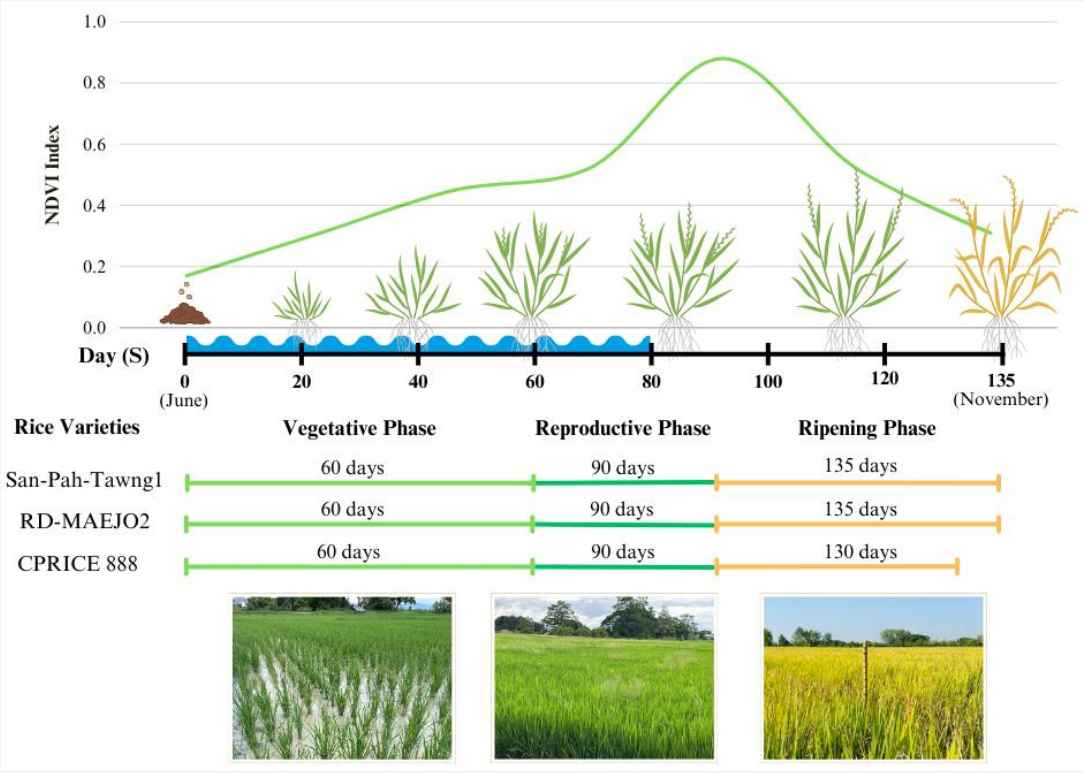

Figure 2: NDVI and growth phases for rice varieties in Buak Khang subdistrict

During the reproductive phase (60-90 days), the NDVI values continue to rise, reaching up to 0.88. As the rice enters the ripening phase (90-135 days), the NDVI values begin to decrease until harvest [17]. In this study, all three rice varieties exhibit similar growth patterns, with slight variations between the different varieties. San-Pah-Tawng1 and RD-MAEJO2 have a total maturation period of 135 days from planting to harvest, while CPRICE 888 has a slightly shorter maturation period of 130 days.

2.4 Multiple Linear Regression Analysis

This research focuses on studying the growth stages of rice, crop health, and yield estimation using Sentinel-1 and Sentinel-2 satellite imagery on the GEE platform. The study integrates field survey data, such as the number of days after rice plantings and yield quantities, with indices derived from analyzing Sentinel-1 and Sentinel-2 satellite images. Statistical analysis tools, particularly MLR, are employed. MLR, an extension of simple linear regression, models the relationship between the dependent variable and two or more independent variables, allowing for a more comprehensive understanding of the factors influencing the dependent variable by considering multiple predictors simultaneously. This versatile and effective tool helps understand and predict outcomes based on multiple predictors [18].

The equation used for the calculations is shown in Equation 1:

$$Y = \beta_0 + \beta_1 X_1 + \beta_2 X_2 + \cdots + \beta_p X_p + \epsilon \quad \text{Equation 1}$$

Where:

Y = Dependent variable, which in this study refers to the number of days after rice plantings and rice yield.

β_0 = Y-intercept.

$X_1, X_2, \cdots, X_p$ = Independent variables, which in this study refer to the parameters of the SAR backscatter coefficients and the indices from Sentinel-2 satellite imagery.

$\beta_1, \beta_2, \cdots, \beta_p$ = Coefficients for the independent variables.

ϵ = Error term.

2.5 Methodology

In the study assessing rice growth stages, crop health, and yield in the Buak Khang Subdistrict, Sentinel-1 SAR GRD images from descending orbits with *VH* and *VV* polarizations, along with Sentinel-2 MSI Level-2A images incorporating the RGB, NIR, and SWIR bands, were employed. Data processing was conducted using the GEE platform.

For Sentinel-1 SAR image processing, the *VV* and *VH* backscatter coefficients were utilized as variables in developing models for evaluating rice growth stages. Sentinel-2 images were used to derive *NDVI*, *NDWI*, and *NDMI* indices for monitoring rice phenology, assessing crop health, and serving as variables for yield estimation. The dataset derived from all analyses was subsequently divided into training (70%) and testing (30%) sets to evaluate the model's accuracy in conjunction with field data. The overall workflow of the methodology is presented in Figure 3.

2.5.1 Data pre-processing

The entire study was conducted on the GEE cloud platform, where the pre-processing of Sentinel-1 and Sentinel-2 data was a crucial step to ensure the highest possible accuracy and consistency of the data used in the analysis. This section summarizes the detailed steps involved in the pre-processing of these satellite datasets. Pre-processing Sentinel-1A Interferometric Wide (IW) Level 1 GRDH images begins with determining the backscatter coefficients in decibels (dB) from each pixel. These backscatter coefficients provide essential information about the surface properties of the rice fields being studied. The data is then filtered using a multi-look speckle filter, which is specifically designed to remove noise caused by speckle, a common issue in radar imagery that can obscure valuable details. This filtering process results in clearer and more reliable data for subsequent analysis. Next, smoothing is performed using a Boxcar kernel. The Boxcar kernel is a type of convolution filter that averages the pixel values within a defined neighborhood, effectively reducing any remaining noise and improving the overall quality of the imagery [19]. For the pre-processing of Sentinel-2 data in GEE, the Harmonized Sentinel-2 MSI images were used, which merge observations from both Sentinel-2A and Sentinel-2B satellites. This ensures consistent data quality and facilitates long-term environmental monitoring. The initial step involves cloud masking, where images with less than 30% cloud cover are selected. Subsequently, atmospheric correction is performed to adjust for atmospheric disturbances, thereby extracting accurate surface reflectance values. Cloud masking effectively removes hazy pixels, and atmospheric correction enhances the precision of surface reflectance values [20] and [21].

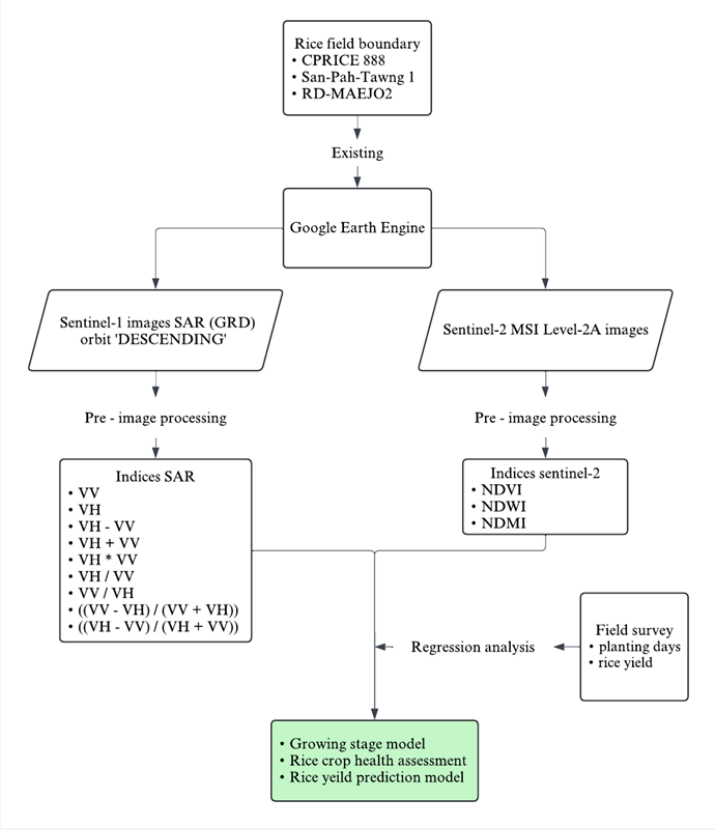

Figure 3: The conceptual framework emphasizes the modeling workflow for assessing rice growth stages, evaluating the abundance of rice crops, and creating models for productivity assessment

2.5.2 Sentinel-1 SAR

Time series data of SAR backscatter coefficients are used to monitor the physiology of rice because SAR data can reveal significant changes in the structure of rice plants, helping to identify key physiological stages. This study utilizes dual-polarization time series data from Sentinel-1 (*VV* and *VH*) to examine the relationship between rice growth parameters and backscatter coefficients. 9 parameters were developed to assess rice growth stages using these backscatter coefficients: *VV* polarization backscatter coefficient, *VH* polarization backscatter coefficient, sum of backscatter coefficients (*VV* + *VH*), product of backscatter coefficients (*VV* × *VH*), difference of backscatter coefficients (*VV* - *VH*), cross-pole ratio of backscatter coefficients (*VV*/*VH*), cross-pole ratio of backscatter coefficients (*VH*/*VV*), and the SAR vegetation index (SVI_1, SVI_2) of backscatter coefficients. This SVI_1 and SVI_2 were developed specifically for this study, based on modifications of the *NDVI* index equation used in optical imagery. They are calculated from the backscatter coefficients of *VV* and *VH* polarizations. The equations for SVI_1 and SVI_2 are similar in form but differ in the emphasis placed on the backscatter coefficients. SVI_1 primarily emphasizes the *VH* backscatter coefficient, which may be beneficial for detecting specific types of vegetation or surfaces. In contrast, SVI_2 focuses on the *VV* backscatter coefficient, which may better characterize certain types of crops than *VH*. Therefore, this study employed both SVI_1 and SVI_2 to effectively highlight the distinctive characteristics and conditions of rice in the study area. The equations used for these calculations are presented in Equations 2 and 3:

$$SVI_1 = \frac{VH - VV}{VH + VV}$$

Equation 2

$$SVI_2 = \frac{VV - VH}{VH + VV}$$

Equation 3

Where:

SVI_1 = The ratio of the difference between *VH* and *VV* to the sum of *VH* and *VV*

SVI_2 = The ratio of the difference between *VV* and *VH* to the sum of *VH* and *VV*

VV = the backscatter coefficient for vertical-vertical polarization.

VH = the backscatter coefficient for vertical-horizontal polarization.

These backscatter coefficient parameters were selected based on previous studies that primarily utilized dual-polarization time series data from *VV* and *VH* for assessing rice growth stages [22][23][24] and [25]. Data collection has shown that *VV* polarization reflectance is sensitive to vertically aligned structures (such as plant stems and tree trunks) and is mainly used to analyze vertical structures. This sensitivity helps in distinguishing changes in vegetation structure over time. On the other hand, VH polarization reflectance is sensitive to targets that cause polarization changes in the reflected wave, such as rough surfaces, heterogeneous environments, or multiple scattering interactions, like in dense forests with complex canopies or certain types of ground cover. In this study, the capabilities of both *VV* and *VH* backscatter coefficients will be tested in evaluating rice growth stages, using parameters that have been studied before as well as those developed specifically for this research. A total of eight parameters are considered, as mentioned above, with details provided in Table 1

Table 1: The parameters used in developing the model to assess the growth stages of rice

Parameters	Definition	Index
Sum of Backscatter Coefficients.	*VV + VH*	*AVV*
Product of Backscatter Coefficients	*VV * VH*	*MVV*
Difference of Backscatter Coefficients	*VV - VH*	*SVV*
Cross-Pole Ratio of Backscatter Coefficients	*VV/VH*	*DVV*
Cross-Pole Ratio of Backscatter Coefficients	*VH/VV*	*DVH*
SVI_1 of Backscatter Coefficients	SVI_1	*IVH*
SVI_2 of Backscatter Coefficients	SVI_2	*IVV*

2.5.3 Spectral indices

Sentinel-2 MSI Level-2A images, including the RGB, NIR, and SWIR bands, are used to analyze the Normalized Difference Vegetation Index (NDVI), Normalized Difference Water Index (NDWI), and Normalized Difference Moisture Index (NDMI) to assess rice plant health, monitor growth stages, and evaluate yield. The NDVI is a widely used spectral index for monitoring vegetation health [26]. It leverages the difference between the visible red and near-infrared bands to measure plant vigor. The formula for NDVI is as follows (Equation 4):

$$NDVI = \frac{NIR - \mathrm{Re}\,d}{NIR + \mathrm{Re}\,d}$$

Equation 4

Where:

NDVI = Normalized Difference Vegetation Index
NIR = Spectral reflectance acquired from near-infrared region
Red = Spectral reflectance acquired from red region

The NDWI is a vital tool used to monitor changes in plant water content [27]. This index is particularly significant for its efficiency in detecting the presence of liquid water within vegetation. Utilizing remote sensing data from the Sentinel-2 satellite, the NDWI focuses on specific spectral bands to provide accurate measurements of water content in plants. Specifically, it makes use of the green and infrared bands, which are sensitive to water content and thus provide reliable data for assessing vegetation health. The formula for calculating the NDWI, which highlights its reliance on the green and infrared bands, is as follows (Equation 5):

$$NDWI = \frac{Green - NIR}{Green + NIR}$$

Equation 5

Where:

NDWI = Normalized Difference Water Index
NIR = Spectral reflectance acquired from near-infrared region
Green = Spectral reflectance acquired from green region

The NDMI is an essential tool for understanding plant water stress and assessing overall plant health [28]. This index provides significant insights into the moisture content of plants, which is a critical factor in determining their growth and productivity. By analyzing the time profile of NDMI, researchers can gain a comprehensive understanding of how moisture content varies across different growth stages of rice. This analysis is crucial as it helps to identify periods of water stress, which can adversely affect the health and yield of the crop. The formula for calculating the NDMI, which is based on the specific spectral bands that are sensitive to moisture content, is as follows (Equation 6):

$$NDMI = \frac{NIR - SWI\,\mathrm{R}1}{NIR + SWI\,\mathrm{R}1}$$

Equation 6

Where:

NDMI = Normalized Difference Moisture Index
NIR = Spectral reflectance acquired from near-infrared region
SWIR = Spectral reflectance acquired from short wave infrared region

2.5.4 Growth stages of rice process

In this study of rice growth stages, research was conducted in Buak Khang Subdistrict, covering the period from planting to harvest, from June to November 2023. The growth stages of rice were divided into three phases: the Vegetative Phase (0 - 60 days), the Reproductive Phase (60 - 90 days), and the Ripening Phase (90 - 135 days). The study focused on utilizing field data on planting and harvesting dates collected from the study area, which was then analyzed alongside remote sensing data. This remote sensing data included backscatter coefficients from Sentinel-1 SAR dual polarization (*VV*, *VH*) and indices from Sentinel-2 satellite imagery at different times. The aim was to determine parameters to analyze the relationship between the number of days of rice cultivation and the backscatter coefficients from Sentinel-1 SAR dual polarization (*VV*, *VH*), using 9 parameters including *VV*, *VH*, *AVV*, *MVV*, *SVV*, *DVV*, *DVH*, *IVV*, *IVH*. Additionally, this study also utilizes 3 parameters derived from indices of Sentinel-2 satellite imagery: *NDVI*, *NDWI*, and *NDMI*. Each index plays a significant role in reflecting various environmental factors that influence rice growth. NDVI provides information about vegetation greenness, indicating plant health; NDWI reflects moisture levels in plants and soil; and NDMI provides information on plant water content. Integrating data from these indices enables remote sensing to offer a comprehensive view of rice crops, covering aspects from leaf vitality and soil moisture to plant water content analysis. This approach is crucial for understanding and managing rice growth at all stages, from planting to harvest. The use of multiple indices enhances the accuracy of monitoring rice growth. These parameters were used to develop a MLR model for assessing rice growth stages. The analysis involved data collected from sample plots and points in the field, combined with Sentinel-1 SAR reflectance parameters and Sentinel-2 indices to create a comprehensive model for evaluating the growth stages of rice.

2.5.5 Crop health assessment

The assessment of rice health was conducted from June to November 2023 during the rainy season. The NDVI, derived from Sentinel-2 images that were corrected and filtered to remove 30% cloud cover,

was used. This index is crucial for evaluating and monitoring the health and density of vegetation. This method is effective with high temporal sampling, allowing the detection of deviations from expected behavior due to factors such as drought, pests, and floods [29]. In this study, four NDVI images were calculated: images from June 3, July 8, September 21, and November 20. However, since most farmers in the study area began planting rice after June 20, the June image could not be used. Additionally, by November, most farmers had completed harvesting, rendering the November image unusable. This study focused on assessing rice health during the Reproductive Phase (60 – 90 days) and the early Ripening Phase (90 – 110 days) before harvest. Therefore, only two images were usable for the assessment. Rice health was evaluated using the maximum and minimum NDVI values in the area.

2.5.6 Rice yield estimation

This study focuses on developing a comprehensive understanding of rice yield by using plot-level yield data collected from detailed field surveys. The primary objective is to analyze the relationship between this yield data and various vegetation indices and backscatter coefficients obtained from satellite imagery. Specifically, the study examines the *NDVI*, the *NDWI*, and the *NDMI* derived from Sentinel-2 satellite imagery. These indices are crucial for assessing plant health, water content, and moisture levels, which are significant factors in understanding crop productivity. Additionally, the study utilizes backscatter coefficients from Sentinel-1 SAR data, including *VV*, *VH*, and combinations such as *AVV*, *MVV*, and *SVV*, as well as ratios like *DVV* and *DVH*. The study also incorporates SVI, calculated as *IVV* and *IVH*. These coefficients and indices provide detailed insights into the structural and compositional characteristics of rice fields, which are vital for yield prediction. The model will be developed using multiple linear regression statistical analysis, which will enable the identification of key parameters that significantly influence rice yield outcomes [30].

2.5.7 Accuracy assessment

The accuracy of the rice growth stage assessment model was rigorously tested by comparing the predicted values with comprehensive field reference data that had been meticulously collected. To ensure a robust evaluation of the model's performance, 75 test sample points were used, representing approximately 30% of the total 250 sample points from the study area. The evaluation process involved using a confusion matrix, a powerful tool for classification analysis, which allowed for the detailed calculation of several key accuracy metrics [31] and [32]. These metrics included the overall accuracy of the model. The accuracy of the rice yield evaluation model was thoroughly examined using reference data from all 44 sample plots within the study area. This comprehensive approach ensured that the evaluation encompassed a wide range of plot conditions and potential yield variations. The accuracy of the yield predictions was measured using the Root Mean Square Error (RMSE) method [18], a standard measure in statistical analysis that provides a clear indication of the model's precision by calculating the average magnitude of the errors between predicted and observed yield values. This systematic accuracy assessment process ensured that both the growth stage and yield evaluation models were rigorously validated.

3. Results and Discussion

3.1 Analysis of Growth Stages Model

This study tested the relationship between various parameters using the reflectance values of sample points and plot samples to identify the best model for evaluating the rice growth stages. The findings indicated that the reflectance values of plot samples exhibited a stronger correlation between parameters compared to those of the sample points. It was also observed that the three parameters calculated from the Sentinel-2 vegetation indices *NDVI*, *NDWI*, and *NDMI* did not show any correlation with the number of days after rice plantings parameters. As a result, these indices were not included in the equation for creating a model to evaluate rice growth stages. Therefore, this study chose to focus only on the reflectance parameters of plot samples that demonstrated a correlation with the number of days after rice plantings parameters. Figure 4 illustrates the results of the relationships between all parameters and the number of days after rice plantings, with the details of the parameters used presented in Table 2. The correlation matrix of the coefficients shows the relationship between the number of days after rice plantings parameters and various other parameters.

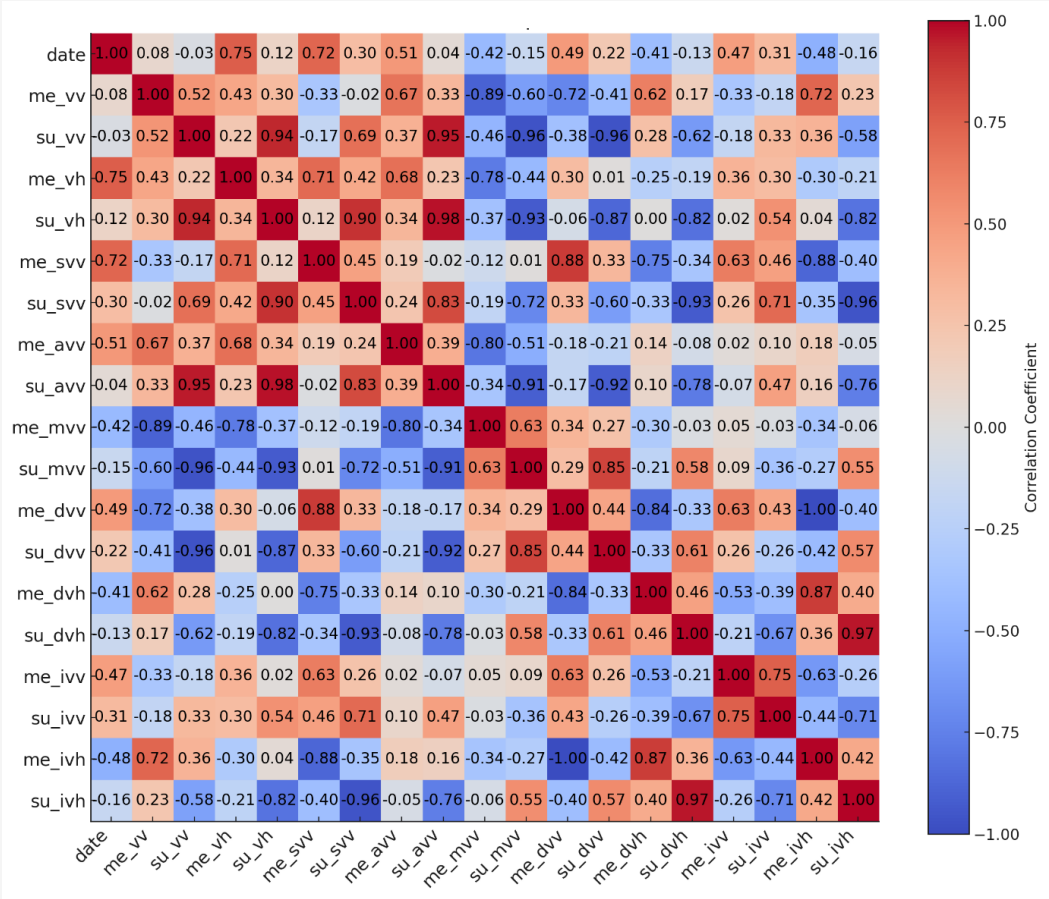

Figure 4: Correlations between the parameters for estimating rice growth stage from reflectance values in sample plots during June – November 2023

It is evident that the parameter for the number of days after rice plantings (*date*) has the highest positive correlation with the parameter *me_vh* (0.75) compared to other parameters. It also shows a positive correlation with parameters *me_svv* (0.72), *me_avv* (0.51), and *me_dvv* (0.49) in descending order. Additionally, the number of days after rice plantings parameter (*date*) exhibits a negative correlation with parameters *me_ivh* (-0.48), *me_dvh* (-0.42), and *me_mvv* (-0.41) respectively. However, these negative correlations still show relatively low levels of association. Moreover, it is observed that most of the parameters correlated with the number of days after rice plantings parameter (*date*) are derived from the average reflectance values in the sample plots. These correlations help identify parameters with clear relationships, whether positive or negative, as well as variables that are relatively independent. When all of this data was applied in stepwise MLR analysis to create a model for assessing rice growth stages, three models were identified with R^2 values greater than 0.5, as shown in Table 3. Model 1 has an R^2 of 0.56 and includes only one predictor, *me_vh*. The standard error of the estimate is 23.153, indicating the average distance between observed and predicted values. Model 2 has an R^2 of 0.64 and includes two predictors: *me_vh* and *me_dvv*. The standard error of the estimate decreases to 20.987, indicating improved predictive accuracy compared to Model 1. Model 3 has an R^2 of 0.67 and includes three predictors: *me_vh*, *me_dvv*, and *me_avv*. The standard error of the estimate decreases slightly compared to Model 2, indicating the best fit and highest predictive accuracy. It is evident that all three rice growth stage assessment models have predictors with positive correlations to the number of days after rice plantings parameter (*date*). However, Figure 4 shows that the parameter *me_svv* has a stronger positive correlation with the number of days after rice plantings (*date*)) than the parameters *me_avv* and *me_dvv*. Nevertheless, *me_svv* was not included in the rice growth stage estimation model because, when considering the mutual correlation between *me_svv* and *me_vh*, it was found that they are highly correlated. This high correlation renders *me_svv* unsuitable for inclusion in the model.

Table 2: Reflectance parameters used to develop a model for assessing rice growth stages

Parameters	Abbreviation
Number of days after rice plantings	*date*
Average *VV* reflectance	*me_vv*
Sum of *VV* reflectance	*su_vv*
Average *VH* reflectance	*me_vh*
Sum of *VH* reflectance	*su_vh*
Average *SVV* reflectance	*me_svv*
Sum of *SVV* reflectance	*su_svv*
Average *AVV* reflectance	*me_avv*
Sum of *AVV* reflectance	*su_avv*
Average *MVV* reflectance	*me_mvv*
Sum of *MVV* reflectance	*su_mvv*
Average *DVV* reflectance	*me_dvv*
Sum of *DVV* reflectance	*su_dvv*
Average *DVH* reflectance	*me_dvh*
Sum of *DVH* reflectance	*su_dvh*
Average *IVV* reflectance	*me_ivv*
Sum of *IVV* reflectance	*su_ivv*
Average *IVH* reflectance	*me_ivh*
Sum of *IVH* reflectance	*su_ivh*

Table 3: Multivariate linear regression modeling for estimation of rice growth stages

Model	Equation	R Square
1	11.708(*me_vh*) + 259.222	0.563
2	10.337(*me_vh*) + 106.695(*me_dvv*) + 179.511	0.642
3	10.337(*me_vh*) + 149.794(*me_dvv*) + 3.365(*me_avv*) + 178.944	0.673

The MLR analysis identified Model 3 as the best model for assessing the growth stages of rice in Buak Khang Subdistrict. This model, which includes the predictors *me_vh*, *me_dvv*, and *me_avv*, achieved an R^2 value of 0.67, demonstrating the highest predictive accuracy among the models tested. The equations derived from the MLR analysis of Model 3 include predictors that are the averages of each parameter (*me_vh*, *me_dvv*, and *me_avv*) of the rice fields in the study area. As a result, the outputs obtained can represent the number of days after rice plantings within the scope of those rice fields. The rice growth stages derived from the equations are divided into three phases: the Vegetative Phase (0–60 days), the Reproductive Phase (60–90 days), and the Ripening Phase (90–135 days). When the equation from Model 3 is used to predict the growth stages of rice using data from satellite imagery dated September 9, 2023 which is a period when the rice fields in the study area are in various growth stages, including the Vegetative Phase, Reproductive Phase, and Ripening Phase the prediction results provide insights into the distribution of the rice growth stages in the study area, as shown in Figure 5. In Figure 5, the growth stages of rice in each plot within the study area are displayed using different colors to specify the growth stages of the rice plants. Light green areas represent the Vegetative Phase, which occurs from 0 to 60 days after planting. During this phase, the rice plants focus on developing roots and stems to build a strong foundation for future growth. Dark green areas indicate the Reproductive Phase, spanning from 60 to 90 days. In this phase, the rice plants begin the processes of flowering and grain production, which are crucial for seed formation and yield. Yellow areas represent the Ripening Phase, the final growth stage occurring from 90 to 135 days after planting. During this phase, the rice grains mature and prepare for harvest. When the results from the model's analysis were used to assess accuracy, a confusion matrix was employed, and the validity was checked by comparing the output of 75 sample points with the corresponding field data. The overall accuracy of the model was found to be 89.8%, indicating that the model effectively classifies the growth stages. The Kappa coefficient was 0.80, reflecting a strong agreement between the predicted classifications and the actual field observations (Table 4).

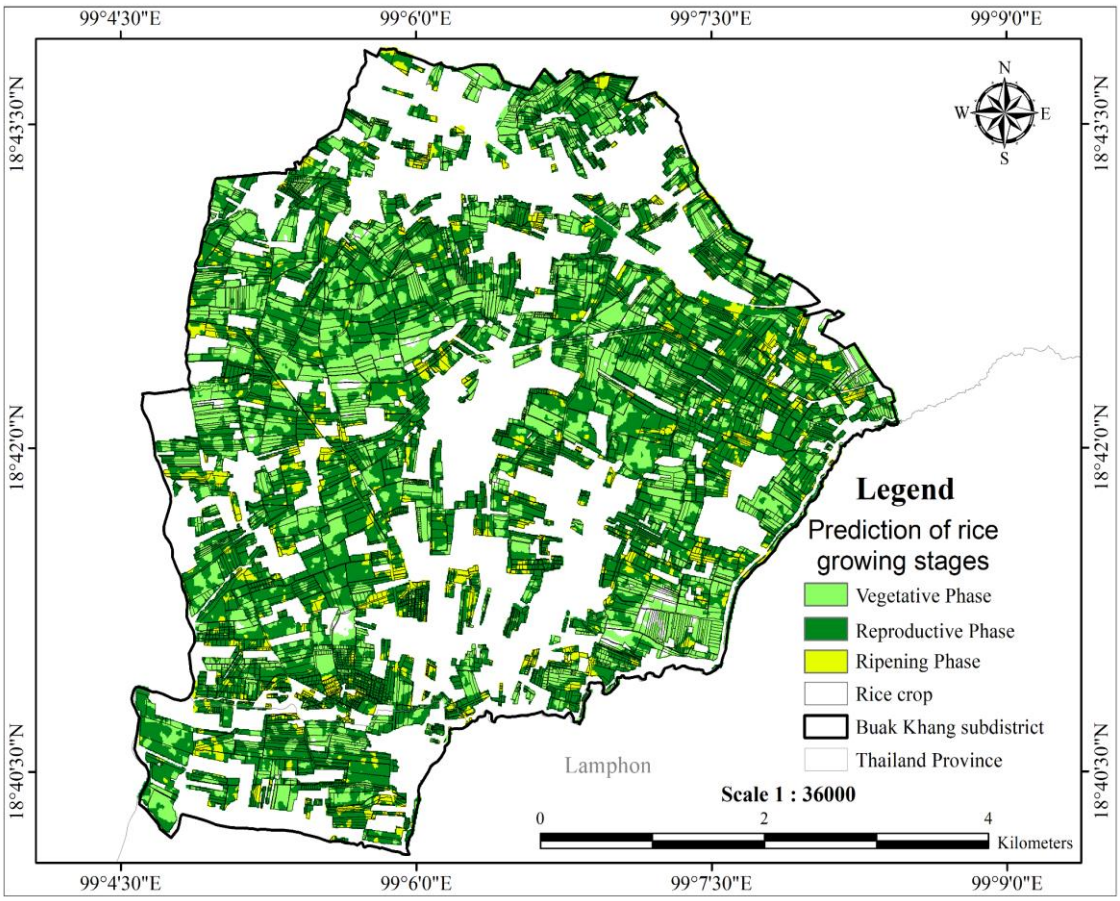

Figure 5: Predicted rice growth stages in Buak Khang subdistrict, Lamphun province, Thailand using A model developed with Sentinel-1 imagery from September 9, 2023

Table 4: Accuracy assessment for the rice growth stage evaluation model using Sentinel-1 SAR satellite imagery from September 9, 2023

		Reference Data				
	Classes	**Vegetative**	**Reproductive**	**Ripening**	**Sum**	**User's Accuracy (%)**
Predicted data	**Vegetative**	47	0	0	47	88.68
	Reproductive	6	92	2	100	91.09
	Ripening	0	9	10	19	83.33
	Sum	53	101	12		
	Producer's Accuracy (%)	95	92	52.63		
	Overall Accuracy (%)		89.8			
	Kappa		0.80			

3.2 Crop Health Assessment

In the study assessing rice health using the NDVI index from Sentinel-2 satellite imagery, it was observed that on July 8, most rice cultivation areas had NDVI values ranging from -0.37 to 0.51 (yellow/brown areas). These reflectance values likely originate from soil and standing water during the Vegetative Phase of rice growth. In July, most farmers in the area were just beginning to plant rice, with the majority of rice plants being between 1 to 50 days old. The areas with NDVI values ranging from -0.37 to 0.51 (yellow/brown areas) correspond to newly planted fields where waterlogging is common, and the rice is in its early growth stages. Additionally, some plots show higher NDVI values (green areas), indicating that the rice is beginning to enter the Reproductive Phase, as shown in Figure 6(a). In the subsequent NDVI image from September 21, it is evident that nearly all the rice fields have significantly higher NDVI values compared to the earlier image from July. Most of the areas are dark green, indicating optimal growth conditions and healthy crops, as most rice fields are at their peak growth stage, as shown in Figure 6(b).

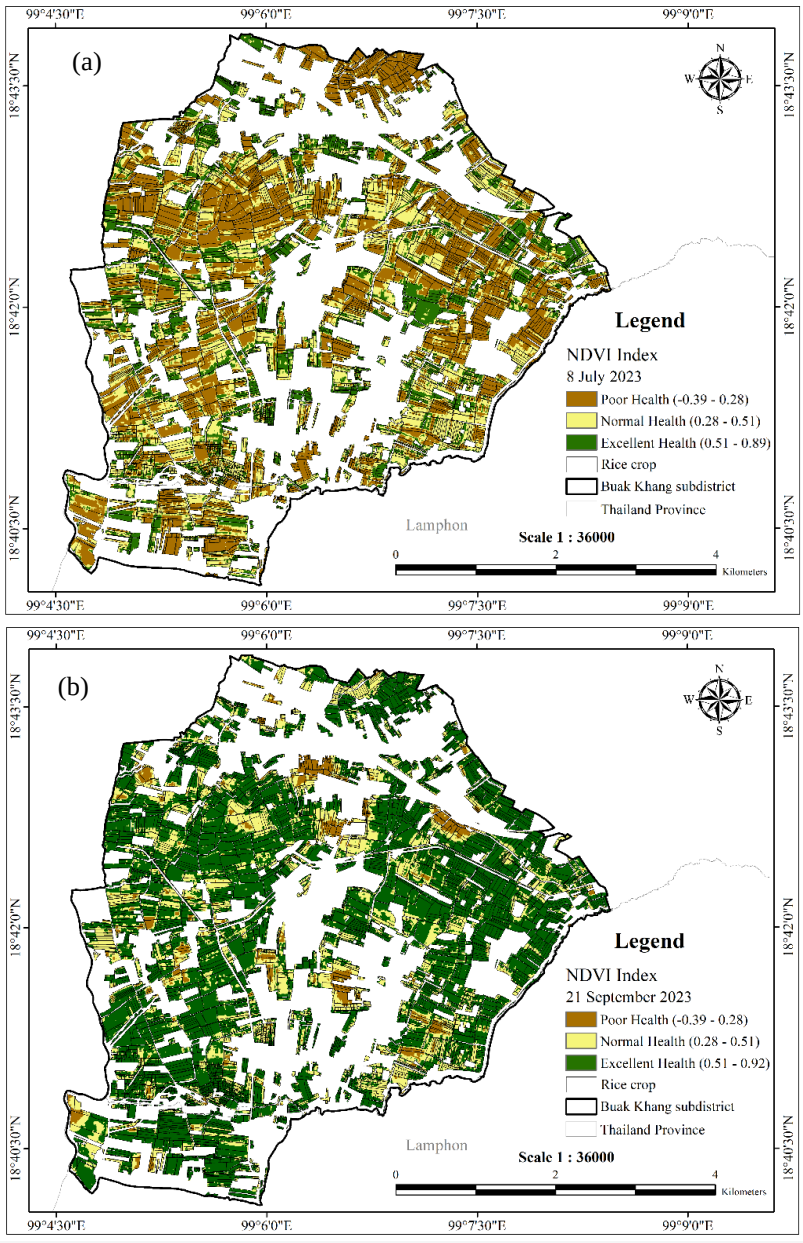

Figure 6: NDVI for rice fields in Buak Khang subdistrict, (a) July 7, and image (b) September 21, 2023

Table 6: Multivariate linear regression modeling for rice yield assessment

Model	Equation	R Square
1	73.528(*mi_SUM*) + 4254.065	0.293
2	77.479(*mi_SUM*) + 44446.376(*wi_MIN*) + 37112.972	0.445
3	68.201(*mi_SUM*) + 50713.833(*wi_MIN*) + 14643.745(*mi_MIN*) + 39247.605	0.515

3.3 Analysis of Rice Yield Model

In this study, the relationships between various environmental parameters and rice yield were evaluated to develop an accurate model for yield estimation. Both sample point and sample plot reflectance values were tested, with the results indicating that sample plot data exhibited stronger correlations among the parameters than sample point data. The parameters analyzed from the sample plots included rice yield (*R_yield*), minimum NDMI (*mi_MIN*), maximum NDMI (*mi_MAX*), mean NDMI (*mi_MEAN*), sum of NDMI (*mi_SUM*), minimum NDWI (*wi_MIN*), maximum NDWI (*wi_MAX*), mean NDWI (*wi_MEAN*), sum of NDWI (*wi_SUM*), minimum NDVI (*vi_MIN*), maximum NDVI (*vi_MAX*), mean NDVI (*vi_MEAN*), and sum of NDVI (*vi_SUM*). The correlation heat map (Figure 7) shows the relationships between the rice yield parameter (R_yield) and other parameters, with correlation coefficients ranging from -1 to 1, where 1 represents a perfect positive correlation, -1 represents a perfect negative correlation, and 0 indicates no correlation. From the analysis of the relationships between the rice yield parameter (*R_yield*) and other parameters, it was found that the parameters *mi_SUM* (0.57), *vi_SUM* (0.55*)*, *wi_MIN* (0.37), and *Mi_MIN* (0.34) have positive correlations with *R_yield*, while the parameter *wi_SUM* (-0.53) has a negative correlation with *R_yield*. By selecting the parameters that are correlated with *R_yield* for analysis using MLR to create a model for estimating rice yield based on parameters derived from indices in Sentinel-2 satellite imagery, a yield estimation model was developed, the details of which are shown in Table 6.

From Table 6, we selected the model with the highest R^2 value for rice yield estimation, which is Model 3 with an R^2 of 0.52. This model includes three predictor variables: *mi_SUM*, *wi_MIN*, and *mi_MIN*. When examining the correlation coefficients between the parameter *R_yield* and other parameters in Figure 7, it was found that these three predictors have positive correlations with *R_yield*. However, even though the parameter *vi_SUM* has a higher positive correlation with *R_yield* than *wi_MIN* and *mi_MIN*, an analysis of the correlations between parameters revealed that *vi_SUM* has a very high positive correlation (0.99) with the parameter *mi_SUM*. Therefore, to avoid redundancy, *vi_SUM* was not included in the yield estimation model. When the equation derived from this model to estimate rice yield, based on Sentinel-2 satellite imagery from September 21, 2023 which is when most of the rice fields in the study area have entered the ripening stage and are ready for harvest in the following month it was found that the parameters in the equations are specific to each area within the rice fields, each area being 100 square meters in size. The resulting outputs display the quantity of rice yield per 100 square meters for each area within the rice fields. More detailed information can be found in Figure 8.

Figure 8 shows rice yield predictions in Buak Khang Subdistrict, with yields presented in kilograms per 100 square meters (kg/100 m^2) and using color shading to represent various yield ranges. This study categorizes yield into three ranges based on actual yield statistics in the study area, from low to high yields. Light green areas represent lower predicted yields, ranging from 0.1768 to 0.7733 kg/m^2, which may indicate suboptimal growth conditions or early stages of plant development. Medium green areas, yielding between 0.7733 and 1.08 kg/m^2, represent medium yields, which may reflect average conditions or growth stages where plants are growing well but not reaching their maximum potential. Yellow areas on the map highlight regions with the highest predicted yields, ranging from 1.08 to 4.522 kg/m^2. Yield in an area depends on the availability of sufficient water, nutrients, and weather conditions during each stage of rice growth. When the results of the yield forecast were used, the accuracy was checked by extracting the results of all 44 predicted points and comparing them with the reference points in the sample plots obtained from field data collection. The yield data was collected in kilograms per rai and converted to kilograms per 100 square meters to match the predicted data. Subsequently, the yield units were converted to kilograms per square meter. When the accuracy was checked using the RMSE method, it was found that the RMSE was 0.887 kg/m^2, which is less than 5%, indicating the model's appropriateness for estimating rice yield in the area.

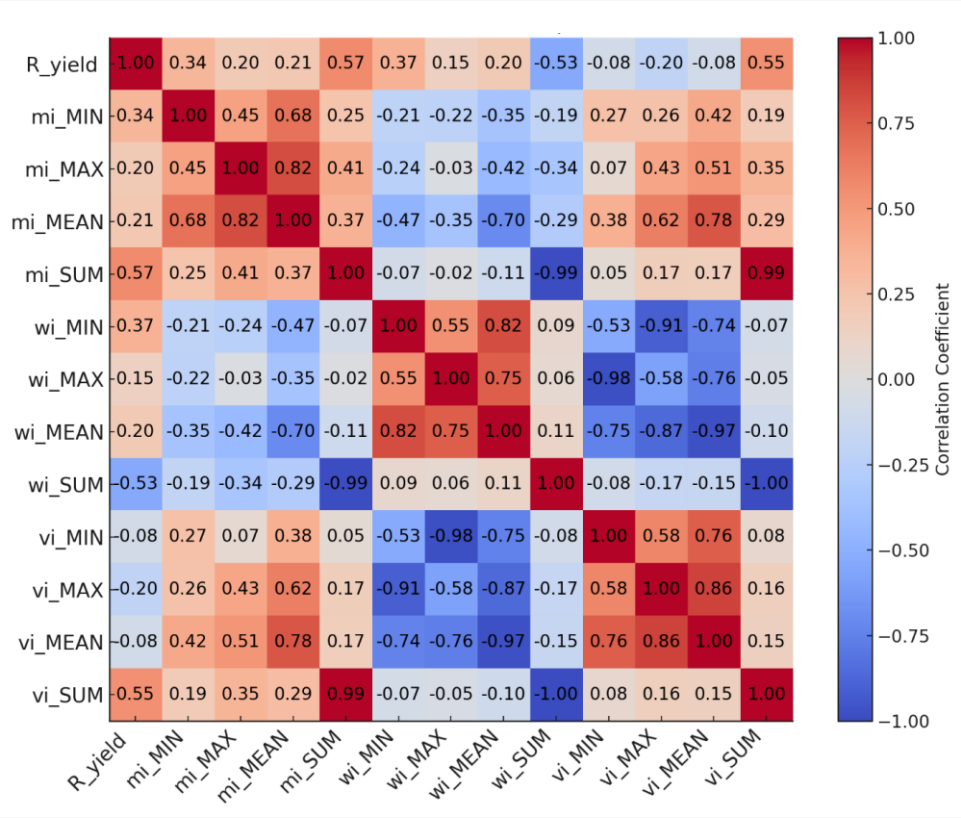

Figure 7: Correlations between rice yield and environmental indices (NDMI, NDWI, NDVI) from sample plot data during June – November 2023

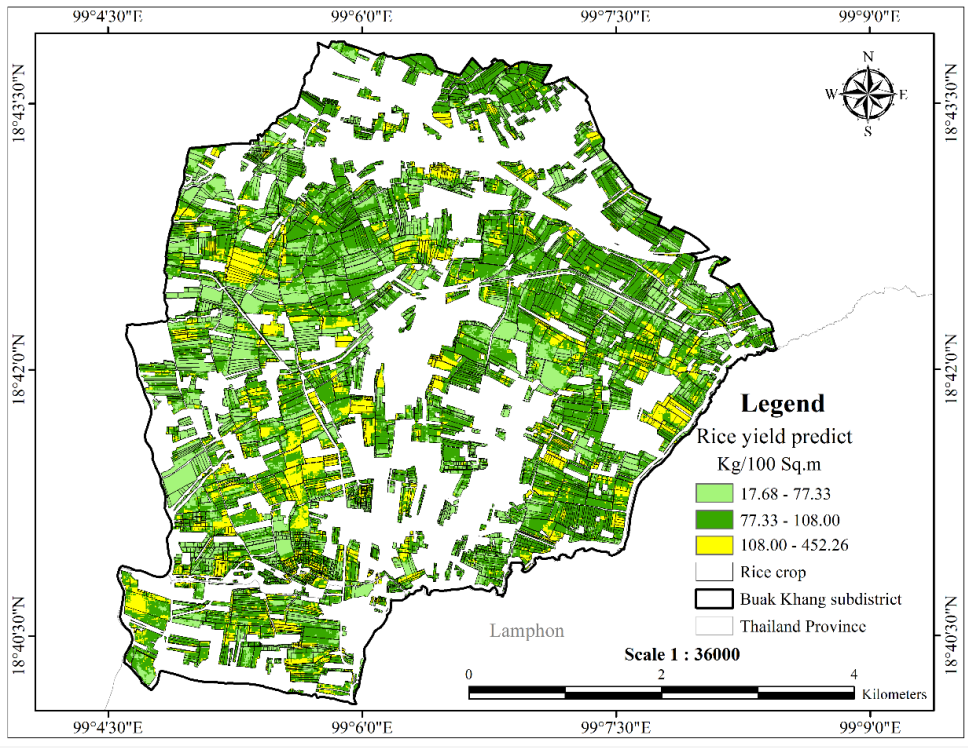

Figure 8: The prediction map of the rice yield in the area of Buak Kang subdistrict, using Sentinel-2 satellite images from September 21, 2023

3.4 Discussion

The study focuses on the use of optical and SAR imagery to model and evaluate rice crop growth stages, health, and yield. Specifically, the research utilizes Sentinel-1 radar and Sentinel-2 optical data to develop models for assessing these parameters, contributing valuable insights into how different satellite data types can be employed to monitor and predict agricultural outcomes under varying environmental conditions. Both optical and radar images were used to identify key parameters for modeling rice growth stages, with the selection process informed by previous studies [4][9][22] and [23]. Notably, the study identified that the most effective model for assessing growth stages was derived solely from Sentinel-1 radar imagery, achieving a Kappa coefficient of 0.8. This finding contrasts with earlier studies that combined data from both Sentinel-1 and Sentinel-2, where the present study's timing during the rainy season limited the usability of Sentinel-2 optical images due to pervasive cloud cover. Consequently, only two usable Sentinel-2 images were available, resulting in a lack of correlation between the radar and optical data. Despite this limitation, the model's Kappa coefficient surpassed those reported in some studies utilizing both optical and radar data [32], underscoring the importance of selecting appropriate data sources based on environmental conditions.

The study also assessed rice crop health using the NDVI. On September 21, the majority of rice fields exhibited NDVI values between 0.51 and 0.92, indicating optimal growth and healthy crops. This finding is consistent with the established literature, which posits that NDVI values above 0.5 and particularly values closer to 1 are indicative of high vegetation health and productivity [2] and [29]. The alignment of these results with previous research reaffirms NDVI as a reliable indicator for evaluating crop health. In terms of yield assessment, the study developed a predictive model using NDVI alongside the NDWI and the NDMI. Contrary to many previous studies that primarily relied on NDVI for yield estimation [1][5][18] and [20], this research found that the inclusion of NDWI and NDMI significantly enhanced the model's predictive accuracy. This divergence from conventional approaches suggests that the effectiveness of various indices can be influenced by factors such as data collection methods, the availability of data types, and the study's timing. Additionally, the study acknowledges the findings of other research that reported no significant correlation between NDVI and yield estimation [33], further emphasizing that the suitability of different indices for yield prediction may be context dependent.

4. Conclusion

The study demonstrates the critical importance of selecting the appropriate type of satellite data and indices for effectively modeling agricultural parameters such as the growth stages, health, and yield of rice crops. The findings reveal that while Sentinel-1 imagery was more reliable for assessing growth stages during the rainy season, health and yield assessments could be improved by considering a combination of indices beyond just NDVI. This underscores the need to adapt data sources and methodologies based on specific environmental conditions and study requirements.

Moreover, the study highlights the variability in research outcomes based on factors such as seasonal timing, data availability, and the specific parameters used in modeling. The discrepancies observed between this study and previous research, particularly in the effectiveness of combined radar and optical data, emphasize the importance of context in remote sensing applications. For instance, the reliance on Sentinel-1 imagery during a season of high cloud cover led to superior model performance, as indicated by a Kappa coefficient of 0.8 for growth stage assessment. In terms of yield prediction, the study found that integrating NDWI and NDMI with NDVI significantly enhanced the model's accuracy, diverging from traditional approaches that prioritize NDVI alone. This finding suggests that the selection of indices should be tailored to the specific agricultural context and study conditions, recognizing that no single index may universally apply across all scenarios. In conclusion, this study reinforces the value of integrating both radar and optical satellite data, along with multiple indices, to improve the accuracy and reliability of remote sensing-based agricultural assessments. The results underscore the necessity of adapting satellite data usage to the environmental context and the specific objectives of the study. These insights contribute to the broader understanding of how satellite-based monitoring can be optimized for better agricultural management and decision-making, particularly in regions with challenging environmental conditions.

For future studies, it would be beneficial to consider comparing the results of the MLR model with other machine learning algorithms, such as Random Forest (RF) and Support Vector Machine (SVM), to improve prediction accuracy. Additionally, for assessing vegetation health, other indices such as the Enhanced Vegetation Index (EVI) and the Soil-Adjusted Vegetation Index (SAVI) should be considered to provide a more comprehensive and accurate evaluation of rice health.

References

[1] Nazir, A., Ullah, S., Saqib, Z. A., Abbas, A., Ali, A., Iqbal, M. S., Hussain, K., Shakir, M., Shah, M. and Butt, M. U., (2021). Estimation and Forecasting of Rice Yield Using Phenology-Based Algorithm and Linear Regression Model on Sentinel-II Satellite Data. *Agriculture*, Vol. 11(10). https://doi.org/10.3390/agriculture11101026.

[2] Tun, S. B. M., Latip, A. S. A., Yacob, N. A. I. and Latif, Z. A., (2022). Crop Monitoring of Paddy Field Using Landsat 8 OLI. *International Journal of Geoinformatics*, Vol.18(4), 35-43. https://doi.org/10.52939/ijg.v18i4.2255.

[3] Kaeomuangmoon, T., Jintrawet, A. and Katzfey, J., (2019). Estimating Seasonal Fragrant Rice Production in Thailand: A Review Article. *International Journal of Agricultural Technology*, Vol. 15(5), 707 - 722.

[4] Suryono, H., Kuswanto, H. and Iriawan, N., (2021). Classification of Paddy Growth Phase with Machine Learning Algorithms to Handle Imbalanced Multi-Class Big Data. *Proceedings of the International Conference on Data Science and Official Statistics*, Vol. 2021(1), 91–100. https://doi.org/10.34123/icdsos.v2021i1.45.

[5] Karnchanasutham, P., Thangtam, N. and Tokitsana, R., (2014). Dry-Season Rice Yield Estimation with SMMS Data by Using Normalize Difference Vegetation Index: A Case Study of Muang District, Suphan Buri Province. *Thai Science and Technology Journal*, 55 - 66. https://li01.tci-thaijo.org/index.php/tstj/article/view/15114/13863.

[6] Choudhary, K., Shi, W., Dong, Y. and Paringer, R., (2022). Random Forest for Rice Yield Mapping and Prediction Using Sentinel-2 Data with Google Earth Engine. *Advances in Space Research*, Vol. 70(8), 2443-2457. https://doi.org/10.1016/j.asr.2022.06.073.

[7] Ni, R., Tian, J., Li, X., Yin, D., Li, J., Gong, H., Zhang, J., Zhu, L. and Wu, D., (2021). An Enhanced Pixel-Based Phenological Feature for Accurate Paddy Rice Mapping with Sentinel-2 Imagery in Google Earth Engine. *ISPRS Journal of Photogrammetry and Remote Sensing*, Vol. 178, 282-296. https://doi.org/10.1016/j.isprsjprs.2021.06.018.

[8] Hashemi, M. G. Z., Abhishek, A., Jalilvand, E., Jayasinghe, S., Andreadis, K. M., Siqueira, P. and Das, N. N., (2022). Assessing the Impact of Sentinel-1 Derived Planting Dates on Rice Crop Yield Modeling. *International Journal of Applied Earth Observation and Geoinformation*, Vol. 114. https://doi.org/10.1016/j.jag.2022.103047.

[9] Fatchurrachman, Rudiyanto, Soh, N. C., Shah, R. M., Giap, S. G. E., Setiawan, B. I. and Minasny, B., (2022). High-Resolution Mapping of Paddy Rice Extent and Growth Stages across Peninsular Malaysia Using a Fusion of Sentinel-1 and 2 Time Series Data in Google Earth Engine. *Remote Sensing*, Vol. 14(8). https://doi.org/10.3390/rs14081875.

[10] Liu, Z., Ju, H., Ma, Q., Sun, C., Lv, Y., Liu, K., Wu, T. and Cheng, M., (2024). Rice Yield Estimation Using Multi-Temporal Remote Sensing Data and Machine Learning: A Case Study of Jiangsu, China. *Agriculture*, Vol. (4). https://doi.org/10.3390/agriculture14040638.

[11] Fu, T., Tian, S. and Zhan, Q., (2023). Phenological Analysis and Yield Estimation of Rice Based on Multi-Spectral and SAR Data in Maha Sarakham, Thailand. *Journal of Spatial Science*, Vol. 69(1), 149-165. https://doi.org/10.1080/14498596.2023.2184428.

[12] Wang, F., Wang, F., Zhang, Y., Hu, J., Huang, J., Xie, L. and Xie, J., (2019). Rice Yield Estimation at Pixel Scale Using Relative Vegetation Indices from Unmanned Aerial Systems. *2019 8th International Conference on Agro-Geoinformatics (Agro-Geoinformatics), Istanbul, Turkey*, 1-4. https://doi.org/10.1109/Agro-Geoinformatics.2019.8820226.

[13] Kulpanich, N., Worachairungreung, M., Thanakunwutthirot, K. and Chaiboonrueang, P., (2023). The Application of Unmanned Aerial Vehicles (UAVs) and Extreme Gradient Boosting (XGBoost) to Crop Yield Estimation: A Case Study of Don Tum District, Nakhon Pathom, Thailand. *International Journal of Geoinformatics*, Vol. 19(20), 65-77. https://doi.org/10.52939/ijg.v19i2.2569.

[14] Setiyono, T., Quicho, E., Gatti, L., Campos-Taberner, M., Busetto, L., Collivignarelli, F., García-Haro, F., Boschetti, M., Khan, N. and Holecz, F., (2018). Spatial Rice Yield Estimation Based on MODIS and Sentinel-1 SAR Data and ORYZA Crop Growth Model. *Remote Sensing*, Vol. 10(2). https://doi.org/10.3390/rs10020293.

[15] Qin, J., Hu, T., Yuan, J., Liu, Q., Wang, W., Liu, J., Guo, L. and Song, G., (2023). Deep-Learning-Based Rice Phenological Stage Recognition. *Remote Sensing*, Vol.15(11). https://doi.org/10.3390/rs15112891.

[16] Zhao, X., Nishina, K., Akitsu, T. K., Jiang, L., Masutomi, Y. and Nasahara, K. N., (2023). Feature-Based Algorithm for Large-Scale Rice Phenology Detection Based on Satellite Images. *Agricultural and Forest Meteorology*, Vol. 329. https://doi.org/10.1016/j.agrformet.2022.109283.

[17] Khoirunnisa, F., Supriatna, and Wibowo, A., (2020). Using NDVI Algorithm in Sentinel-2A Imagery for Rice Productivity Estimation (Case Study: Compreng Sub-district, Subang Regency, West Java). *IOP Conference Series: Earth and Environmental Science*, Vol. 481. https://doi.org/10.1088/17551315/481/1/012064.

[18] Setiyono, T., Quicho, E., Gatti, L., Campos-Taberner, M., Busetto, L., Collivignarelli, F., García-Haro, F., Boschetti, M., Khan, N., and Holecz, F. (2018). Spatial Rice Yield Estimation Based on MODIS and Sentinel-1 SAR Data and ORYZA Crop Growth Model. *Remote Sensing*, Vol. 10(2). https://doi.org/10.3390/rs10020293.

[19] Dineshkumar, C., Kumar, J. S. and Nitheshnirmal, S., (2019). Rice Monitoring Using Sentinel-1 Data in the Google Earth Engine Platform. *Proceedings*, Vol. 24(1). https://doi.org/10.3390/IECG2019-06206.

[20] Soriano-González, J., Angelats, E., Martínez-Eixarch, M. and Alcaraz, C., (2022). Monitoring Rice Crop and Yield Estimation with Sentinel-2 Data. *Field Crops Research*, Vol. 281. https://doi.org/10.1016/j.fcr.2022.108507.

[21] Claverie, M., Ju, J., Masek, J. G., Dungan, J. L., Vermote, E. F., Roger, J.-C., Skakun, S. V. and Justice, C., (2018). The Harmonized Landsat and Sentinel-2 Surface Reflectance Data Set. *Remote Sensing of Environment*, Vol. 219, 145-161. https://doi.org/10.1016/j.rse.2018.09.002.

[22] Xie, G. and Niculescu, S., (2022). Mapping Crop Types Using Sentinel-2 Data Machine Learning and Monitoring Crop Phenology with Sentinel-1 Backscatter Time Series in Pays de Brest, Brittany, France. *Remote Sensing*, Vol. 14(18). https://doi.org/10.3390/rs14184437.

[23] Bhogapurapu, N., Dey, S., Bhattacharya, A., Mandal, D., Lopez-Sanchez, J. M., McNairn, H., López-Martínez, C. and Rao, Y. S., (2021). Dual-Polarimetric Descriptors from Sentinel-1 GRD SAR Data for Crop Growth Assessment. *ISPRS Journal of Photogrammetry and Remote Sensing*, Vol.178, 20-35. https://doi.org/10.1016/j.isprsjprs.2021.05.013.

[24] Mansaray, L. R., Zhang, D., Zhou, Z. and Huang, J., (2017). Evaluating the Potential of Temporal Sentinel-1A Data for Paddy Rice Discrimination at Local Scales. *Remote Sensing Letters*, Vol. 8(10), 967-976. https://doi.org/10.1080/2150704x.2017.1331472.

[25] Singha, C. and Swain, K. C., (2023). Rice Crop Growth Monitoring with Sentinel 1 SAR Data Using Machine Learning Models in Google Earth Engine Cloud. *Remote Sensing Applications: Society and Environment*, Vol. 32. https://doi.org/10.1016/j.rsase.2023.101029

[26] Sukojoa, B. M. and Kurniawan, R. H., (2021). Rice Growth Stages Mapping with Normalized Difference Vegetation Index (NDVI) Algorithm Using Sentinel-2 Time Series Satellite Imagery. *International Journal on Advanced Science Engineering Information Technology*, Vol. 11(4), 1594-1598. https://doi.org/http://dx.doi.org/10.18517/ijaseit.11.4.12335.

[27] Gao, B. C., (1996). NDWI-A Normalized Difference Water Index for Remote Sensing of Vegetation Liquid Water from Space. *Remote Sensing of Environment*, Vol. 58(3), 257-266. https://doi.org/10.1016/s0034-4257(96)00067-3.

[28] Badrul Hisham, N. H., Hashim, N. I., Saraf, N. M. and Talib, N., (2022). Monitoring of Rice Growth Phases Using Multi-Temporal Sentinel-2 Satellite Image. *IOP Conference Series: Earth and Environmental Science, 8th International Conference on Geomatics and Geospatial Technology (GGT 2022)*, Vol. 1051(1). https://doi.org/10.1088/1755-1315/1051/1/012021.

[29] Kaushik, S. K., Mishra, V. N., Punia, M., Diwate, P., Sivasankar, T. and Soni, A. K., (2022). Crop Health Assessment Using Sentinel-1 SAR Time Series Data in a Part of Central India. *Remote Sensing in Earth Systems Sciences*, Vol. 4(4), 217-234. https://doi.org/10.1007/s41976-021-00064-z.

[30] Rananavare, L. B. and Chitnis, S., (2023). Crop Yield Prediction Using Satellite Imagery. *2023 7th International Conference on Computation System and Information Technology for Sustainable Solutions (CSITSS)*, 1-6. http://doi.org/10.1109/CSITSS60515.2023.10334198

[31] Rudiyanto, Minasny, B., Shah, R. M., Che Soh, N., Arif, C. and Indra Setiawan, B., (2019). Automated Near-Real-Time Mapping and Monitoring of Rice Extent, Cropping Patterns, and Growth Stages in Southeast Asia Using Sentinel-1 Time Series on a Google Earth Engine Platform. *Remote Sensing*, Vol. 11(14). https://doi.org/10.3390/rs11141666.

[32] Ramadhani, F., Pullanagari, R., Kereszturi, G. and Procter, J., (2020). Automatic Mapping of Rice Growth Stages Using the Integration of SENTINEL-2, MOD13Q1, and SENTINEL-1. *Remote Sensing*, Vol.12(21). https://doi.org/10.3390/rs12213613.

[33] Boldbaatar, E., (2022*). Crop Yield Estimation Using Sentinel-2 Data: A Case Study from Ugtaaltsaidam Sub-Province, Mongolia.* GRÓ Land Restoration Training Programme [Final project]. https://www.grocentre.is/static/gro/publication/849/document/boldbaatar2022.pdf.